Biochimica et Biophysica Acta 1827 (2013) 1309–1319

Contents lists available at ScienceDirect

Biochimica et Biophysica Acta

journal homepage: www.elsevier.com/locate/bbabio

Review

Design and use of photoactive ruthenium complexes to study electron transfer within cytochrome bc_1 and from cytochrome bc_1 to cytochrome c ☆

Francis Millett [a,*], Jeffrey Havens [a,1], Sany Rajagukguk [b], Bill Durham [a,2]

[a] Department of Chemistry and Biochemistry, University of Arkansas, Fayetteville, AR 72701, USA
[b] San Francisco VA Medical Center, 4150 Clement Street, 151NC, San Francisco, CA, 94121, USA

ARTICLE INFO

Article history:
Received 14 June 2012
Received in revised form 29 August 2012
Accepted 3 September 2012
Available online 15 September 2012

Keywords:
Cytochrome bc_1
Cytochrome c
Electron transfer
Ruthenium

ABSTRACT

The cytochrome bc_1 complex (ubiquinone:cytochrome c oxidoreductase) is the central integral membrane protein in the mitochondrial respiratory chain as well as the electron-transfer chains of many respiratory and photosynthetic prokaryotes. Based on X-ray crystallographic studies of cytochrome bc_1, a mechanism has been proposed in which the extrinsic domain of the iron–sulfur protein first binds to cytochrome b where it accepts an electron from ubiquinol in the Q_o site, and then rotates by 57° to a position close to cytochrome c_1 where it transfers an electron to cytochrome c_1. This review describes the development of a ruthenium photooxidation technique to measure key electron transfer steps in cytochrome bc_1, including rapid electron transfer from the iron–sulfur protein to cytochrome c_1. It was discovered that this reaction is rate-limited by the rotational dynamics of the iron–sulfur protein rather than true electron transfer. A conformational linkage between the occupant of the Q_o ubiquinol binding site and the rotational dynamics of the iron–sulfur protein was discovered which could play a role in the bifurcated oxidation of ubiquinol. A ruthenium photoexcitation method is also described for the measurement of electron transfer from cytochrome c_1 to cytochrome c. This article is part of a Special Issue entitled: Respiratory Complex III and related bc complexes.

1. Introduction

The cytochrome bc_1 complex (cyt bc_1) (ubiquinone:cytochrome c oxidoreductase) is the central integral membrane protein in the mitochondrial respiratory chain as well as the electron transfer chains of many respiratory and photosynthetic prokaryotes [1,2]. The overall net reaction catalyzed by cyt bc_1 involves the 2-electron oxidation of ubiquinol (QH_2) to ubiquinone (Q), and the reduction of two molecules of cytochrome c (Cc). The energy of electron transfer is coupled to the uptake of two protons from the inside of the membrane, and the release of four protons to the outside of the membrane (Eq. (1)):

$$QH_2 + 2\ Cc^{3+} + 2H^+_{in} \rightarrow Q + 2\ Cc^{2+} + 4\ H^+_{out}. \quad (1)$$

Mitochondrial cyt bc_1 is a homodimer with 11 polypeptide chains, while prokaryotic cyt bc_1 complexes contain as few as 3 polypeptide chains [1,2]. Cyt bc_1 contains three redox proteins: cyt b with two b hemes (b_L and b_H), the Rieske iron–sulfur protein (ISP) containing a 2Fe2S cluster, and cyt c_1 with one c-type heme. In the widely accepted Q-cycle mechanism, QH_2 binds to the Q_o site near the outside of the membrane and transfers its first electron to the Rieske iron–sulfur center 2Fe2S, which is then transferred to cyt c_1 and finally to Cc [1–4]. The second electron is transferred from semiquinone in the Q_o site to cyt b_L, and then to cyt b_H and ubiquinone in the Q_i site to form semiquinone. The cycle is repeated to reduce semiquinone in the Q_i site to QH_2. X-ray crystallographic studies have shown that the conformation for the extrinsic domain of the Rieske iron–sulfur protein depends on the crystal form and the presence of Q_o site inhibitors [5–8]. In crystals of cyt bc_1 from all species grown in the presence of stigmatellin, the ISP is in a conformation with 2Fe2S close to the cyt b_L heme, called the b state [5–11] (Fig. 1). In contrast, the ISP is in a conformation with 2Fe2S close to cyt c_1, called the c_1 state, in native chicken or beef $P6_522$ crystals in the absence of inhibitors [6,7]. The intensity of the anomalous signal for 2Fe2S close to cyt b_L is small in bovine $I4_122$ crystals in the absence of inhibitors,

Abbreviations: Cc, cytochrome c; yCc, yeast Cc; cyt bc_1, cytochrome bc_1; CcO, cytochrome c oxidase; 2Fe2S, Rieske iron–sulfur center; ISP, iron–sulfur protein; bpy, 2,2′-bipyridine; dmb, 4,4′-dimethyl-2,2′-bipridine; bpz, 2,2′-bipyrazine; bpd, 3,3′-bipyridazine; qpy, 2,2′:4′,4″:2″,2‴-quaterpyridine; Ru_2D, $[Ru(bpy)_2]_2qpy^{4+}$; *R. sphaeroides*, *Rhodobacter sphaeroides*; MOAS, methoxyacrylate stilbene; JG144, S-3-anilino-5-methyl-5-(4,6-difluorophenyl)-1,3-oxazolidine-2,4-dione; Q, ubiquinone; QH_2, ubiquinol; Q_o, outside ubiquinol binding site; Q_i, inside ubiquinone binding site; P_f, Q_o site inhibitor which fixes ISP in b state; P_m, Q_o site inhibitor which promotes mobile state of ISP

☆ This article is part of a Special Issue entitled: Respiratory complex III and related bc complexes.

* Corresponding author. Tel.: +1 479 575 4999; fax: +1 479 575 4049.
E-mail addresses: millett@uark.edu (F. Millett), jahavens@uark.edu (J. Havens), sany.rajagukguk@gmail.com (S. Rajagukguk), bdurham@uark.edu (B. Durham).
[1] Tel.: +1 479 575 4601; fax: +1 479 575 4049.
[2] Tel.: +1 479 575 7945; fax: +1 479 575 4049.

0005-2728/$ – see front matter © 2012 Elsevier B.V. All rights reserved.
http://dx.doi.org/10.1016/j.bbabio.2012.09.002

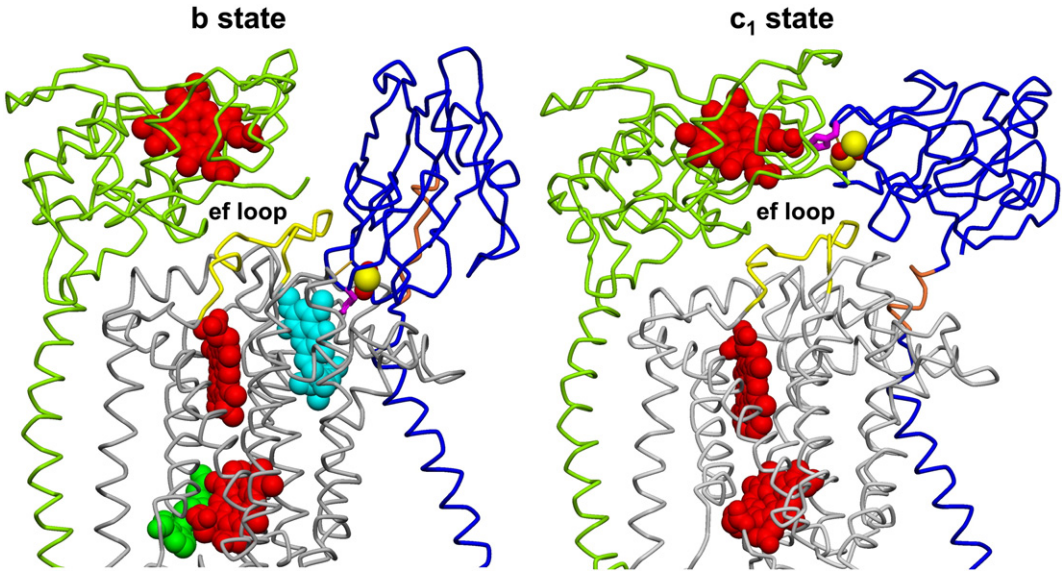

Fig. 1. X-ray crystal structure of chicken cyt bc_1 in *b* state in the presence of stigmatellin and antimycin (PDB: 3H1I) [6], and of beef $P6_5$ 22 crystals in c_1 state (PDB: 1BE3) [7]. The ISP, cyt c_1 and cyt *b* subunits are colored blue, green, and gray, respectively. The hemes, 2Fe2S, stigmatellin, and antimycin are colored red, yellow, cyan, and green. The Rieske neck region residues 66–72 are colored orange, and the *ef* loop residues 252–268 are colored yellow.

indicating that the ISP is conformationally mobile (5,8). A rotational shuttle mechanism involving the extrinsic domain of the ISP has been proposed that is supported by these structural studies (Fig. 1, Scheme 1) [5–8]. QH_2 in the Q_o site transfers an electron to the oxidized 2Fe2S center of the ISP in the *b* state, followed by rotation of the ISP to the c_1 state and electron transfer from reduced 2Fe2S to cyt c_1. This mobile shuttle mechanism is supported by extensive mutational, cross-linking, and kinetic studies [12–28].

An important goal is to measure the rate constants for all of the electron-transfer reactions in cyt bc_1, as well as the dynamics of the conformational changes of the extrinsic domain of the ISP. This has been a challenging goal, since many of the electron-transfer reactions are very rapid. This review describes the development and use of a ruthenium photooxidation technique to study electron transfer in cytochrome bc_1 with microsecond time resolution [13]. This technique has been used to study the key electron-transfer steps in the mechanism of cyt bc_1 as well as the dynamics of the ISP extrinsic domain rotation.

2. Design of photoactive ruthenium complexes

Ruthenium polypyridine complexes have a number of remarkable properties that make them excellent photoredox initiators [29]. They have a long-lived metal-to-ligand charge-transfer excited state that is both a strong oxidant and a strong reductant, and are very stable in both the ground state and the excited state. Ruthenium complexes can be used to rapidly photoreduce or photooxidize neighboring redox centers. In the photooxidation mechanism of Scheme 2, the excited state Ru(II*) accepts an electron from Fe(II) to form Ru(I)–Fe(III) with rate constant k_3. A sacrificial electron acceptor A can oxidize Ru(I) to Ru(II) with rate constant k_8, preventing the k_4 back reaction to Ru(II)–Fe(II). All three chelating ligands of ruthenium can be altered to tune the redox potentials over a wide range, and optimize the rate and yield of photooxidation or photoreduction. The effects of different ligands on the redox potentials of the ruthenium complexes are shown in Table 1. The $Ru(bpz)_2(dmb)$ complex is particularly well-suited for photooxidation applications. We have introduced four different strategies for specifically labeling proteins with photoredox active ruthenium polypyridyl complexes [30–37]. The most useful method involves the formation of a thioether link between a protein cysteine residue and a ruthenium complex containing a bromomethyl group on the heterocyclic ring [34–37]. The location of the cysteine residue on the protein can be genetically engineered to address specific questions [30–37]. We have recently designed binuclear ruthenium complexes which bind non-covalently to C*c*O and cyt bc_1 and initiate photoinduced electron transfer [13,38,39]. $[Ru(bpy)_2]_2(qpy)^{4+}$ (Ru_2D) (Fig. 2) has a net charge of +4 which allows it to bind strongly to the acidic domain on cyt bc_1 and photooxidize cyt c_1 with a yield of 25% according to Scheme 2 [13].

Extensive studies on a wide range of ruthenium-labeled proteins have provided important information on the dependence of electron transfer on driving force, distance and pathway [40–49]. The theory

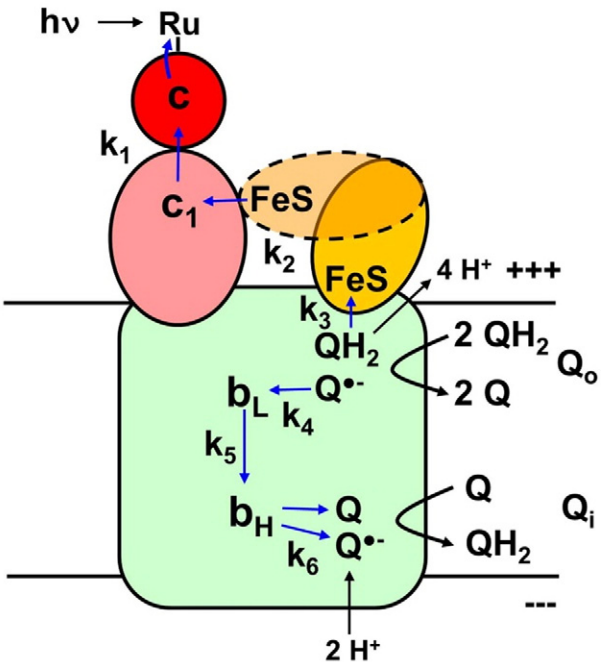

Scheme 1. Photoinduced electron transfer in Ru-Cc – cyt bc_1 complex.

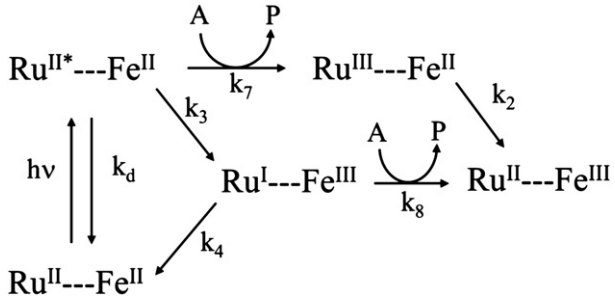

Scheme 2. Photooxidation of cyt c_1 by Ru_2D.

Table 1
Standard reduction potentials (in V) of ruthenium complexes vs. normal hydrogen electrode.

Complex	(II)/(III)	(II*)/(III)	(II)/(I)	(II*)/(I)
$Ru(bpy)_3$	1.27	−0.87	−1.31	0.83
$Ru(bpy)_2(dmb)$	1.27	−0.83	−1.36	0.79
$Ru(bpz)_2(dmb)$	1.76	−0.25	−0.79	1.22
$Ru(bpd)_2(dmb)$	1.49	−0.49	−1.00	0.98

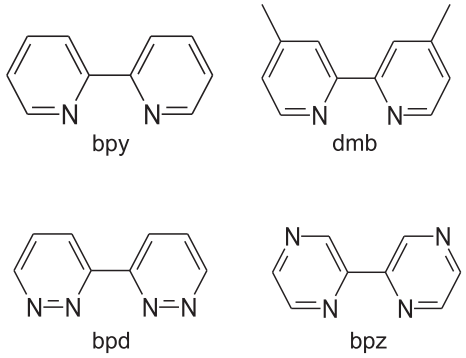

developed by Marcus has revealed that three important factors control the rate of electron transfer, the free energy change $\Delta G^{o\prime}$ of the redox reaction, the reorganization energy λ, and the electronic coupling between the redox centers [50]. The reorganization energy λ is a measure of the energy required to rearrange and repolarize the reactants and surrounding solvent before electron transfer can occur. Dutton and coworkers have reported that the rate constants in a broad range of biological systems can be described approximately by a simple exponential dependence on the distance between the redox centers, as originally proposed by Marcus [51]:

$$k_{et} = k_o \exp[-\beta(r-r_o)] \exp\left[\left(-(\Delta G^{o\prime}+\lambda)^2/4\lambda RT\right)\right] \quad (2)$$

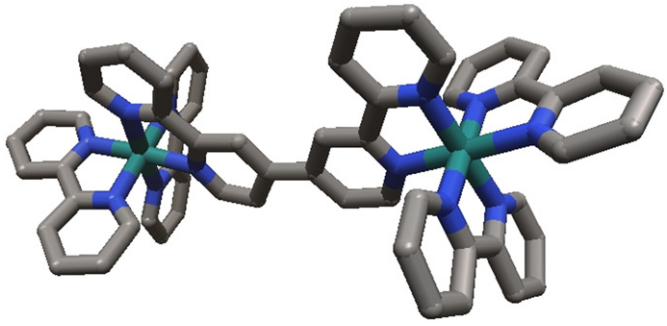

Fig. 2. Modeled structure of Ru_2D. The carbons are colored gray, the nitrogens are blue, and the rutheniums are green.

where r is the distance between the closest macrocycle atoms in the two redox centers, the van der Waals contact distance $r_o = 3.6$ Å, $\beta = 1.4$ Å^{-1}, and the nuclear frequency $k_o = 10^{13}$ s^{-1}.

3. Kinetics of electron transfer within cytochrome *bc*$_1$

The electron-transfer reactions of mitochondrial cyt bc_1 has been studied extensively by stopped-flow spectroscopy and rapid-mix/freeze-quench EPR [52,53]. In the absence of inhibitors, the reduction of heme b_H by ubiquinol in bovine cyt bc_1 is multiphasic. The fast phase is inhibited by antimycin, indicating that it occurs through the Q_i site. The reduction of heme b_H by 300 μM duroquinol through the Q_o site in the presence of antimycin occurred with a half-time of 25 ms, while cyt c_1 and the 2Fe2S center were also reduced with the same half-time, indicating that they are in rapid equilibrium [53]. A rapid technique using photo-releasable decylubiquinol was also used to study reduction of heme b_H and cyt c_1 [54]. In another study, it was found that the rate of reduction of yeast cyt bc_1 by menaquinol was significantly decreased by antimycin, suggesting that the redox states of heme b_L and heme b_H control the reduction of the 2Fe2S center [55]. The effects of Q_o and Q_i site inhibitors on the kinetics of yeast cyt bc_1 led Trumpower to propose an alternating, half-of-the-sites mechanism [56].

A photoexcitation method has been developed to study the kinetics of cyt bc_1 electron transfer in chromatophores of photosynthetic bacteria including *Rhodobacter sphaeroides* and *Rhodobacter capsulatus* [57]. Photoexcitation of the photosynthetic reaction center rapidly oxidizes cyt c_2, which diffuses to cyt bc_1 and oxidizes cyt c_1 with a half-time of 150 μs [58,59]. Cyt c_1 then oxidizes the 2Fe2S center, allowing bifurcated electron transfer from QH_2 in the Q_o site to 2Fe2S and heme b_L and heme b_H. The following rate constants, which are identified in Scheme 1, have been estimated for the cyt bc_1 reactions in *R. sphaeroides* chromatophores: $k_1 > 10^4$ s^{-1} for electron transfer from cyt c_1 to Cc, $k_2 > 10^5$ s^{-1} for electron transfer from 2Fe2S to cyt c_1, $k_3 = 1650$ s^{-1} for electron transfer from QH_2 to 2Fe2S in the Q_o site, $k_4 > 10^9$ s^{-1} for electron transfer from $Q^{\bullet-}$ to heme b_L in the Q_o site, $k_5 > k_3$, and $k_6 > k_3$ [59]. Shinkarev et al. [60] have determined that electron transfer between cyt b_L and cyt b_H has a half-time of 0.1 ms using the transient electric field generated by excitation of the reaction center to initiate reverse electron transfer from cyt b_H to cyt b_L.

A laser flash photolysis method was developed to study electron transfer within the cyt bc_1 complex using the binuclear ruthenium complex Ru_2D [13] (Schemes 2, 3). *R. sphaeroides* cyt bc_1 is typically redox poised with cyt c_1 and 2Fe2S reduced, heme b_L oxidized, and heme b_H and quinol partially reduced (Scheme 3). Laser excitation of Ru_2D to the metal-to-ligand charge transfer state, Ru_2D^*, a strong oxidant, leads to oxidation of cyt c_1 within 700 ns, as indicated by the rapid decrease in the reduced cyt c_1 absorbance band at 552 nm (Fig. 3). A sacrificial electron acceptor A such as $[Co(NH_3)_5Cl]^{2+}$ is present in the solution to oxidize Ru^{II*} and/or Ru^{I} and promote oxidation of cyt c_1 by either of the pathways shown in Scheme 2. The +4 charge on Ru_2D allows it to bind selectively to the negatively charged domain on the surface of cyt c_1 with a dissociation constant of 8 μM [13]. The photooxidation of cyt c_1 is complete within 670 ns, the lifetime of the Ru_2D excited state, indicating that Ru_2D must be very close to cyt c_1 at the time of the flash [13,61]. Ru_2D does not photooxidize other proteins that do not have a negatively charged domain, such as cytochrome *c*, and does not photooxidize the iron–sulfur center, cyt b_L, or cyt b_H in cyt bc_1 [61].

The photooxidation of cyt c_1 by Ru_2D^* is followed by biphasic reduction of cyt c_1 with rate constants of 80,000 s^{-1} and 2000 s^{-1} (Fig. 3) [13]. The fast phase has been assigned to electron transfer from reduced 2Fe2S to photooxidized cyt c_1 with rate constant k_2, while the slow phase of cyt c_1 reduction is correlated with the oxidant-induced reduction of heme b_H, monitored at 561–569 nm (Fig. 3). The oxidant-induced reduction of cyt b_H is rate-limited by transfer of the first electron from QH_2 to

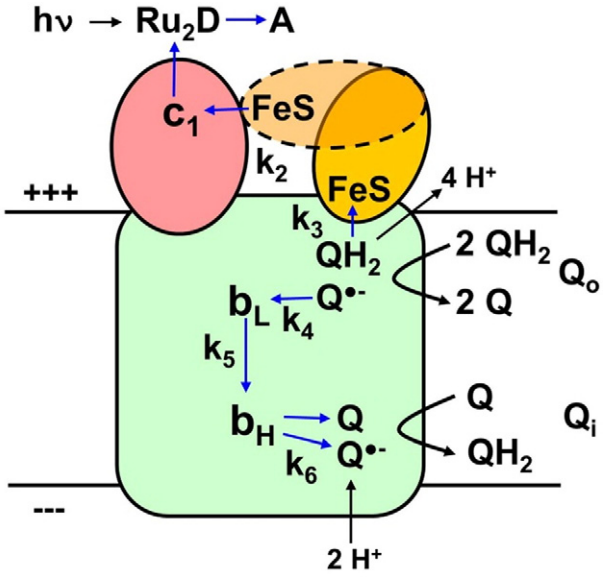

Scheme 3. Electron transfer in cyt bc_1 photoinduced by Ru_2D.

2Fe2S with rate constant k_3. The subsequent transfer of the second electron from the semiquinone to heme b_L and heme b_H with rate constants k_4 and k_5 is much more rapid than k_3, and not rate-limiting. The kinetics of both electron transfer from 2Fe2S to cyt c_1 and from QH_2 to 2Fe2S can thus be resolved by this technique. Electron transfer in the bovine cyt bc_1 complex and *Paracoccus denitrificans* cyt bc_1 has also been studied using this technique [13,61]. The rate constants for bovine cyt bc_1 are $k_2 = 16{,}000\ s^{-1}$ and $k_3 = 250\ s^{-1}$, while for the *P. denitrificans* complex they are $k_2 = 10{,}700\ s^{-1}$ and $k_3 = 700\ s^{-1}$.

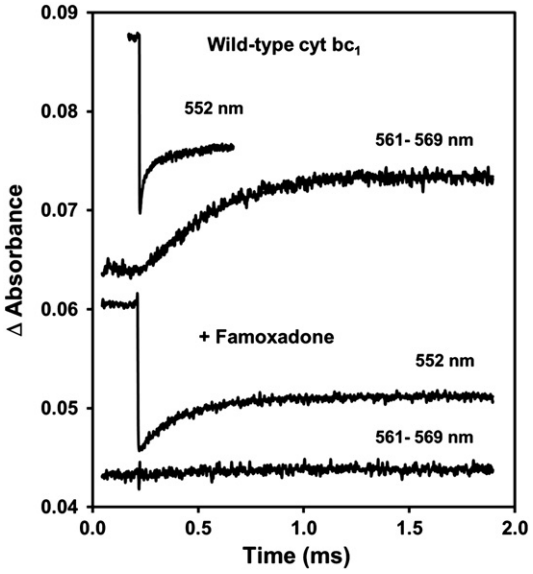

Fig. 3. Electron transfer within wild-type *R. sphaeroides* cyt bc_1 initiated by photooxidation of cyt c_1 [68]. The sample contained 5 μM cyt bc_1, 20 μM Ru_2D, 5 mM $[Co(NH_3)_5Cl]^{2+}$, in 20 mM sodium borate, pH 9.0 with 0.01% dodecylmaltoside. Treatment of cyt bc_1 with 10 μM $Q_oC_{10}BrH_2$, 1 mM succinate, and 50 nM SCR completely reduced 2Fe2S and cyt c_1, and reduced cyt b_H by 30%. Cyt c_1 was photooxidized within 1 μs, and then reduced with rate constants of 80,000 s^{-1} and 2000 s^{-1}, as indicated in the 552 nm transient. The rate constant for the reduction of cyt b_H measured at 561–569 nm was 2300 s^{-1}. (Bottom two traces) Addition of 30 μM famoxadone decreased the rate of reduction of cyt c_1 to 5400 s^{-1} and eliminated reduction of cyt b_H.

An important question is whether the rate constant k_2 for electron transfer from 2Fe2S to cyt c_1 is rate-limited by true electron transfer, proton gating, or conformational gating [21]. The most definitive way to discriminate between true electron transfer and conformational gating mechanisms is by changing the driving force of the reaction, since Marcus theory predicts a large dependence of the rate of true electron transfer on driving force. The redox potential of 2Fe2S is decreased significantly as the pH is increased from pH 7.0 to pH 10.0 due to the deprotonation of the 2Fe2S ligand His-161, leading to an increase in the driving force $\Delta G^{o\prime}$ from −0.02 V to +0.115 V [62,63]. However, the rate constant k_2 for electron transfer from 2Fe2S to cyt c_1 in *R. sphaeroides* cyt bc_1 was independent of pH, even though Marcus theory predicts that the rate constant should increase 12-fold as the pH is increased from 7.0 to 10.0 [21]. This Marcus theory calculation using Eq. (2) is based on the assumption that $\lambda = 1.0$ V. Although λ has not been measured for this reaction, a value of 1.0 V is typical for cytochromes with a similar heme solvent exposure to that of cyt c_1 [21,43,49]. Moreover, the rate constant k_2 was not affected by the ISP mutations Y156W, S154A, and Y156F/S154A which decrease the redox potential of 2Fe2S by 62 mV, 109 mV, and 159 mV, respectively (Table 2) [21]. Marcus theory, Eq. (2), predicts that the increase in the driving force in these mutants would increase the rate constant by up to 17-fold (Table 2), assuming $\lambda = 1.0$ V [21]. These studies indicate that the rate constant k_2 for electron-transfer from the 2Fe2S center to cyt c_1 is controlled by conformational gating rather than the rate of transfer of the electron. For this conformational gating mechanism to be valid, the fluctuations in the conformation of the Rieske iron–sulfur protein must be slow compared to electron transfer in the active c_1 state. A model for the active c_1 state is provided by the bovine $P6_522$ crystal structure [6,7], in which the 2Fe2S ligand His-161 forms a hydrogen bond with the heme c_1 propionate oxygen (Fig. 4). There is a pathway for electron transfer from the 2Fe2S center to heme c_1 that has a distance of 7.8 Å from the His-161 nitrogen to the closest heme c_1 macrocycle atom C3D (Fig. 4). Eq. (1) predicts a rate constant k_2 ranging from 1.5×10^6 to $3\times10^7\ s^{-1}$ for this pathway, assuming λ values between 1.0 and 0.7 eV, which are typical for cytochromes [43,49]. The observed rate constant k_2 for electron transfer from 2Fe2S to cyt c_1 is considerably smaller than the predicted value for the c_1 state, consistent with a conformational gating mechanism.

A central question about the bifurcated reaction at the Q_o site is how QH_2 can deliver 2 electrons sequentially to the high and low potential chains, while avoiding short-circuit and bypass reactions. It has been proposed that the controlled motion of the ISP extrinsic domain may play a role in a gating mechanism for the electron bifurcation reaction at the Q_o site [10,12,28]. X-ray crystallography studies have shown that inhibitors bound at the Q_o site have a significant influence on the position and mobility of the ISP. Binding P_m type inhibitors such as myxothioazol to the Q_o site lead to the release of ISP from the *b*-state to a disordered "mobile" state not detected in the crystal, while structures complexed with P_f type inhibitors such as stigmatellin show that ISP binds to the *b* subunit in a "fixed" state [8,10,25,28]. EPR studies have also provided valuable information on the effect of Q_o site

Table 2
Kinetic properties of *R. sphaeroides* cyt bc_1 mutants [21]. Enzymatic activity in μmol cyt *c* reduced/min/μmol cyt *b* at 25 °C. ΔE_m is the difference in redox potential between 2Fe2S and cyt c_1 at pH 8.0, 25 °C. k_2 is the experimental rate constant for electron transfer from 2Fe2S to cyt c_1 at pH 8.0, 25 °C. Theoretical rate constant for electron transfer is calculated from Eq. (2) with r = 9.9 Å, λ = 1.0 eV, and ΔG^o calculated from the ΔE_m value of the mutant cyt bc_1.

Mutant	Enzymatic activity	ΔE_m (mV)	k_2 ($10^4\ s^{-1}$) (experimental)	k_2 ($10^4\ s^{-1}$) (theory)
Wild-type	2.5	0	8.0	8.0
Y156W	0.58	−62	15.0	26.0
S154A	0.23	−109	7.8	60.0
S154A/Y156F	0.03	−159	9.0	140.0

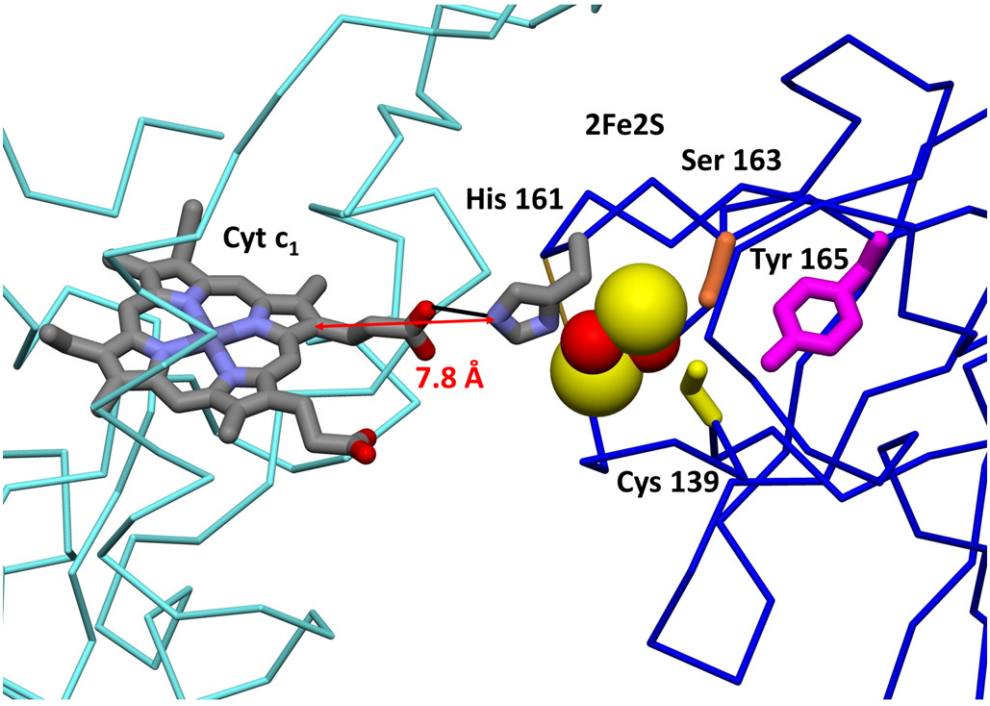

Fig. 4. Structure of bovine cyt bc_1 P6$_5$22 crystals in the c_1 state (PDB: 1BE3) [7]. The Rieske and cyt c_1 subunits are colored dark blue and light blue, respectively, the 2Fe2S center is shown as a CPK model colored red/yellow, and heme c_1 is colored by element. His-161, Ser-163,Tyr-165, and Cys-139 are shown as sticks. The hydrogen bond between the Nε2 nitrogen of His-161 and the heme c_1 propionate oxygen is shown with a line. The distance of 7.8 Å from the His-161 nitrogen to the closest heme c_1 macrocycle atom C3D is indicated by the red arrow. Tyr-165 and Ser-163 in the bovine ISP are homologous to Tyr-156 and Ser-154 in the *R. sphaeroides* ISP.

inhibitors on the position and orientation of the ISP [17,22,26,27]. Havens et al. [61] have studied the effects of six different Q_o site inhibitors on electron transfer from ISP to cyt c_1 in *P. denitrificans* cyt bc_1 using the Ru_2D photooxidation technique. Binding any of the P_m inhibitors MOA-stilbene, myxothiazol, or azoxystrobin to cyt bc_1 increased the rate and extent of electron transfer from ISP to cyt c_1, consistent with release of ISP from the *b* state which causes a linked decrease in the redox potential and increase in the mobility of the ISP (Table 3). Binding the P_f inhibitor stigmatellin completely prevented electron transfer from ISP to cyt c_1, consistent with X-ray crystallography studies showing that stigmatellin locks the ISP in the *b*-state with a hydrogen bond between a carbonyl group of the inhibitor and His-161, a ligand of the 2Fe2S cluster [8,10,64–66]. In contrast, binding the P_f type inhibitors JG-144 and famoxadone decreased the rate constant by 5 to 10-fold, and increased the amplitude over 2-fold. These inhibitors therefore do not lock the ISP in the *b* state, but rather decrease the rate of its release from the *b* state and rotation to the c_1 state. Binding reduced QH_2 leads to a two-fold increase in the amplitude of the fast phase, A_{1f}. These results indicate that the species occupying the Q_o site has a significant effect on the dynamics of the ISP domain rotation.

Table 3
Effects of Q_o site inhibitors on electron transfer in *P. denitricans* cyt bc_1 [61]. k_{2f} and A_{2f} are the rate constant and amplitude of the fast phase of electron transfer between 2Fe2S and cyt c_1, respectively. Solutions contained 5 μM cyt bc_1, 20 μM Ru_2D, 1 mM ascorbate, 4 μM TMPD, and 5 mM $[Co(NH_3)_5Cl]^{2+}$ in 20 mM Tris–HCl pH 8.0. Inhibitor concentrations were 25 μM.

Inhibitor/substrate	Type	k_{2f} (s^{-1})	A_{2f}
None	–	6300	10%
MOAS	P_m	9900	33%
Myxothiazol	P_m	8900	30%
Azoxystrobin	P_m	8000	28%
Stigmatellin	P_f	0	0
JG-144	P_f	1300	16%
Famoxadone	P_f	600	26%
Q	–	5300	10%
QH_2	–	10,700	18%

X-ray crystallography studies of bovine cyt bc_1 have shown that binding P_f type inhibitors such as famoxadone displace the cd1 helix and the *ef* helix away from each other to widen the Q_o pocket and form a binding crater for the capture of the ISP in the *b*-state (Figs. 5, 6) [28]. Photoactivated ruthenium kinetic studies have shown that famoxadone binding does not completely immobilize the ISP in the *b* state, but rather slows down the rate of its release and rotation to the c_1 state. Famoxadone binding to bovine cyt bc_1 decreased k_2 from 16,000 s^{-1} to 1500 s^{-1}, while in *R. sphaeroides* cyt bc_1 k_2 was decreased from 60,000 s^{-1} to 5400 s^{-1} [67] (Fig. 3). A series of mutants at residues in the *ef* loop were constructed to explore the role of the *ef* loop in regulating the dynamics of the ISP [68] (Table 4; Fig. 5). The mutation Y280A caused a decrease in k_2 from 60,000 s^{-1} to 7900 s^{-1}, but famoxadone binding only decreased k_2 to 3200 s^{-1}. Similarly, the I292A mutation decreased k_2 to 4400 s^{-1}, but famoxadone binding only decreased it to 3000 s^{-1}. These mutations might cause a conformational change similar to that of famoxadone, limiting the additional effect of famoxadone binding. The I292A mutation caused a decrease in the rate constant k_3 for electron transfer from QH_2 to 2Fe2S from 2300 s^{-1} to 350 s^{-1}, indicating an effect on the conformation of the QH_2 reaction site. Mutation of L286A at the tip of the *ef* loop had an interesting effect, decreasing k_2 to 33,000 s^{-1} and k_3 to 740 s^{-1}. However, famoxadone binding does not lead to any further decrease in k_2, suggesting that this mutation might block the famoxadone-induced conformational change in the wild-type protein. Darrouzet et al. have also carried out experiments indicating the importance of L286 [18,23].

Extensive research has been carried out on the bifurcated electron transfer reaction at the Q_o site where QH_2 transfers the first electron to the ISP and cyt c_1, and the resulting semiquinone transfers the second electron to cyt b_L and cyt b_H [28,69–79]. Potential mechanisms

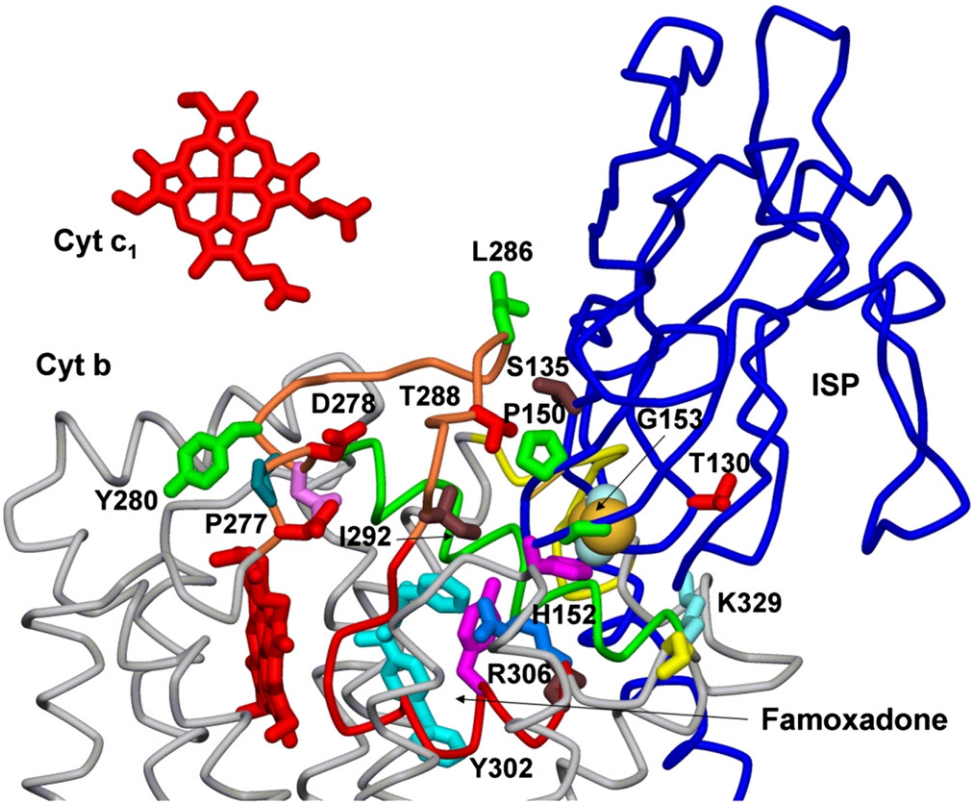

Fig. 5. X-ray crystal structure of bovine cyt bc_1 in the presence of famoxadone (PDB: 1LOL) [58]. Famoxadone is colored cyan, the cyt c_1 and cyt b_L hemes are red, and the 2Fe2S center is represented by a CPK model. The ISP is blue, and cyt *b* is gray. Residues 252–268 in the *ef* loop are colored orange while residues 269–283 in the PEWY sequence and the *ef* helix are red. Residues 136–152 in the cd1 helix are green and residues 163–171 in the neck-contacting domain are colored yellow. Residues of interest are indicated by sticks, and labeled with *R. sphaeroides* sequence numbering.

must be consistent with the reversibility of the reaction, and prevent short-circuit reactions, including the delivery of both electrons from ubiquinol to 2Fe2S and cyt c_1 in the high potential chain. Double gating mechanisms have been proposed in which QH_2 can only react if *b*-state ISP and cyt b_L are both initially oxidized [69,76–79]. Crofts and colleagues have proposed a coulombic gating mechanism in which the semiquinone anion moves from the distal site near the ISP to a site near oxidized cyt b_L in a process controlled by electrostatics [71,77]. Another possibility is simultaneous transfer of two electrons from QH_2 to the ISP and cyt b_L in a concerted reaction without the formation of a semiquinone intermediate [69,76,78–80]. However, a semiquinone radical at the Q_o site has been detected at the Q_o site by two different methods [81,82], and a semiquinone is also thought to be required in the bypass reaction during formation of superoxide [83].

Unfortunately, it has not been possible to experimentally detect QH_2 or Q in the Q_o binding pocket by X-ray crystallography. However, the effects of Q_o site inhibitors on the structural linkage between the conformations of cyt *b* and the ISP have led to a proposal for the mechanism for bifurcated electron transfer [12,28]. It was proposed that binding QH_2 to the Q_o site widens the Q_o pocket between the cd1 helix and *ef* helices forming a crater to bind the ISP in the *b*-state (Fig. 6) [12,28]. This would promote the formation of a hydrogen bond between QH_2 and His-161 and lead to proton-coupled electron transfer from QH_2 to oxidized 2Fe2S. After the second electron was transferred from semiquinone to cyt b_L and cyt b_H, the resulting oxidized Q would leave the distal Q_o binding pocket, triggering the cd1 and *ef* helices to come closer together and release the ISP from the docking crater, allowing it to rotate to the c_1 position and transfer an electron to cyt c_1 [12,28]. The effects of P_m and P_f inhibitors on the rapid kinetics of bovine, *R. sphaeroides*, and *P. denitiricans* cyt bc_1 provide evidence that the conformations of the Q_o site, the ISP docking crater, and the ISP extrinsic domain orientation and dynamics are tightly linked. It is suggested that binding P_f inhibitors to the Q_o site leads to a conformation similar to that of the active QH_2–oxidized ISP complex, while binding P_m inhibitors leads to a conformation in which the ISP is released from the *b*-state to a mobile state. The linkage between the Q_o site and the ISP conformation and dynamics may play an important role in gating the electron transfer bifurcation reaction in the Q_o site to minimize short-circuit and bypass reactions. Other factors are also likely to be involved in gating, including coulombic gating of the motion of the semiquinone [72,77], and the conformations of water or amino acid side chains in the Q_o pocket [69,75–79]. There is also evidence that events at the Q_i site and the b_L and b_H hemes might be linked to turnover at the Q_o site [26,27,84–89]. In addition, conformational interactions and electron transfer between the two monomers of the cyt bc_1 dimer might play a role in the mechanism of the reaction at the Q_o site [85,89–92].

4. Reaction between Cytochrome bc_1 and Cytochrome c

Cytochrome *c* is a hydrophilic heme protein with a molecular weight of 12,500 Da that transfers electrons from the cyt bc_1 complex to cytochrome *c* oxidase by a diffusional shuttle mechanism. The electron-transfer reaction from the cyt bc_1 complex to C*c* involves three steps: a) formation of a 1:1 reactant complex between reduced cyt bc_1 and Cc^{3+}, *b*) intracomplex electron transfer from cyt c_1^{2+} to Cc^{3+}, and *c*) release of the product Cc^{2+}. The overall rate of the reaction is optimized when the interaction between C*c* and cyt bc_1 stabilizes a reactant complex which allows rapid electron transfer, and also promotes rapid reactant complex formation and product

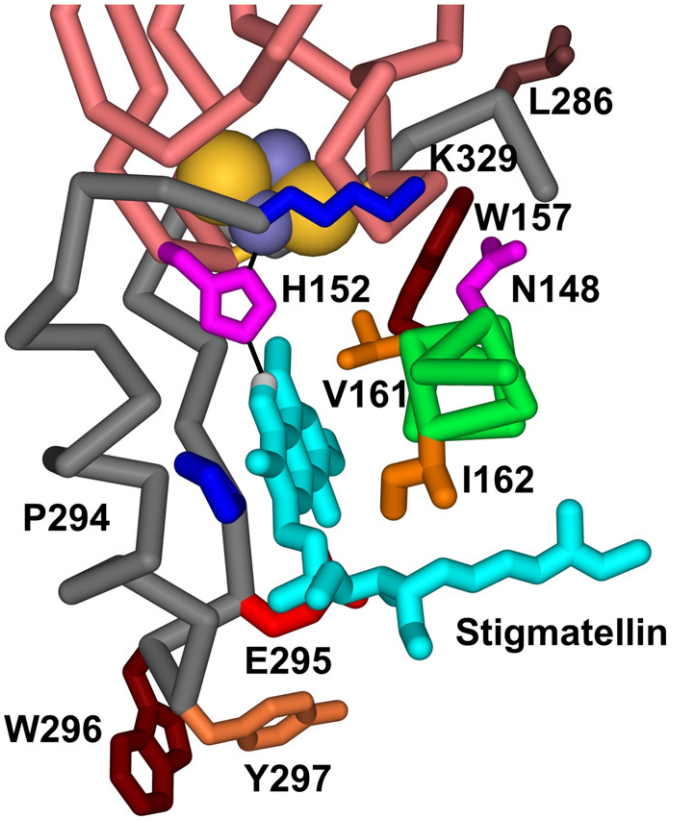

Fig. 6. X-ray crystal structure of ISP bound to the docking crater on cyt b with stigmatellin bound to bovine cyt bc_1 (PDB:1SQX) [28]. View is parallel to membrane, showing *ef* loop and helix (gray), cd1 helix (green), and ISP (orange). The H-bond between stigmatellin and the His-152 ligand to 2Fe2S is shown with a line. Residues on cyt b near the Q_o site or interacting with the ISP are shown as sticks, and labeled with *R. sphaeroides* sequence numbering.

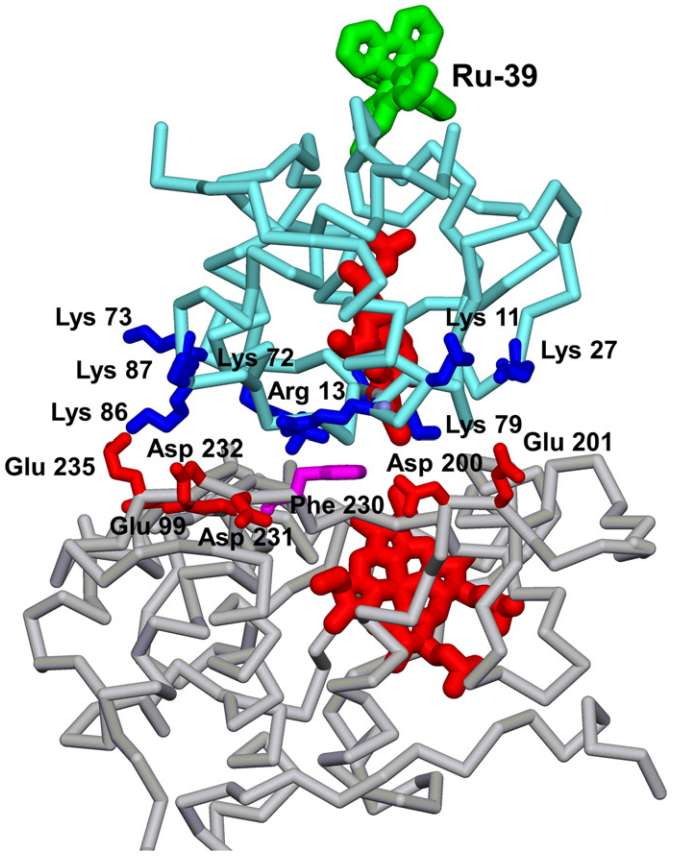

Fig. 7. X-ray crystal structure of the complex between yeast cyt bc_1 and yC*c* [99] (PDB: 1KYO). yC*c* is colored light blue, Cyt c_1 is gray, the heme groups are red, basic residues on yC*c* are blue, acidic residues on cyt c_1 are red, and Phe-230 is purple. The ruthenium complex on Cys-39 (green) was attached to the crystal structure by molecular modeling.

complex dissociation. The steady-state reaction rate decreases with increasing ionic strength, indicating the involvement of electrostatic interactions between the two proteins [93–95]. Extensive chemical modification studies have demonstrated that six lysine amino groups surrounding the heme crevice of C*c* are involved in binding to cyt bc_1 [93–96]. Chemical modification and cross-linking studies have shown that acidic residues on cyt c_1 and subunit 8 in bovine cyt bc_1 are involved in binding C*c* [97,98]. X-ray crystal structures of beef, chicken, yeast, and *R. sphaeroides* cyt bc_1 reveal that the cyt c_1 heme edge on the cytoplasmic surface is surrounded by acidic residues that could form a binding site for C*c* [5–9]. Most importantly, the X-ray crystal structure of the complex between yeast C*c* and yeast cyt bc_1 revealed that it is stabilized by non-polar interactions at the center of the binding domain, including a planar stacking interaction between yC*c* Arg-13 and Phe-230 of cyt c_1 (Fig. 7) [99,100]. There are only two direct polar interactions in the binding domain, but additional charged residues around the periphery of the binding domain may contribute to the electrostatic interaction. The distance between the edges of the heme *c* and heme c_1 groups is 9.4 Å.

Stopped-flow spectroscopy has been used to measure the second-order electron transfer reaction between C*c* and bovine cyt c_1 at high ionic strength, but the reaction becomes too fast to resolve by this technique below 200 mM ionic strength [52]. In *R. sphaeroides* chromatophores, the reaction is rate-limited by the diffusion of photooxidized cyt c_2 from the reaction center to the cyt bc_1 complex with an apparent rate constant of 5000 s^{-1} [58,59]. These techniques have provided valuable information about the reaction between cyt c_1 and C*c*, but it was not possible to measure the intracomplex rate constant.

It was necessary to design a new ruthenium-labeled C*c* derivative to study rapid electron transfer from cyt bc_1 to C*c* in the forward, physiological direction. A brominated $Ru(bpz)_2(dmb)$ reagent was used to label the Cys-39 sulfhydryl group on yeast H39C,C102T C*c* to form Ru_z-39-C*c* (Fig. 7) [101]. The ruthenium complex is on the surface opposite from the heme crevice of C*c*, and does not affect the interaction with yeast cyt bc_1. There is an efficient pathway for electron transfer between the heme and the ruthenium complex consisting of 13 covalent bonds and one hydrogen bond, with a distance of 12.6 Å. The new $Ru(bpz)_2(dmb)$ complex has a reduction potential of 1.22 V for the $Ru(II^*)/Ru(I)$ transition. The driving force of 1.0 V for the $Ru(II^*)$–$Fe(II) \rightarrow Ru(I)$–Fe(III) reaction is close to the expected reorganization energy λ of 0.8 V, which should allow optimal photooxidation of the reduced heme *c* according to Scheme 2.

Table 4
Effect of mutations on electron transfer within *R. sphaeroides*. cyt bc_1 [68]. The rate constant k_2 for electron transfer from 2Fe2S to cyt c_1 was measured in a solution containing 5 μM cyt bc_1, 20 μM Ru_2D, 5 mM $[Co(NH_3)_5Cl]^{2+}$, in 20 mM sodium borate, pH 9.0, 0.01% dodecylmaltoside. The cyt bc_1 was treated with 10 μM $Q_oC_{10}BrH_2$, 1 mM succinate, and 50 nM SCR to completely reduce 2Fe2S and cyt c_1, and reduce cyt b_H by about 30%. Famoxadone (30 μM) was added where indicated. The rate constant k_3 for electron transfer from QH_2 in the Q_o site to 2Fe2S was measured without famoxadone.

Mutant	Activity	k_2 (s^{-1})	k_2 (s^{-1}) with famoxadone	k_3 (s^{-1})
WT	2.35	60,000	5400	2300
Y280A (*b*)	1.34	7900	3200	2800
L286A (*b*)	0.78	33,000	35,000	740
I292A (*b*)	0.81	4400	3000	350
P150C (ISP)	0.23	50,000	2000	4
G153C (ISP)	0.78	13,000	1470	450

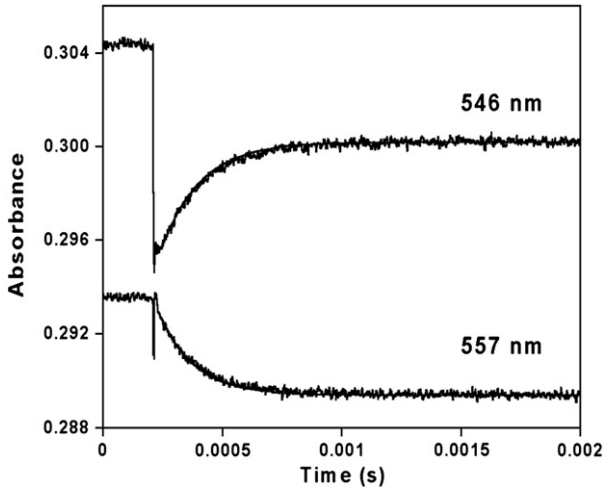

Fig. 8. Photoinduced electron transfer between yeast Ru-39-C*c* and yeast cyt bc_1 [101]. The solution contained 5.2 μM yeast Ru_z-39-C*c* and 4.4 μM yeast cyt bc_1 in 5 mM sodium phosphate, pH 7.0, 250 mM NaCl, and 0.1% lauryl maltoside. It was treated with 2 μM TMDP and 10 μM ascorbate to reduce the c_1 and *c* hemes. The 550 nm transient shows the photooxidation and reduction of Ru-39-C*c*, while the 557 nm transient shows the oxidation of cyt c_1. The transients at both wavelengths indicate electron transfer from cyt c_1 to C*c* with a rate constant of $3900 \pm 600\ s^{-1}$.

The photoinitiated electron transfer from heme *c* Fe(II) to Ru(II*) in Ru_z-39-C*c* occurred with a rate constant of $k_3 = 1.5 \times 10^6\ s^{-1}$, followed by back electron transfer from Ru(I) to Fe(III) with a rate constant of $k_4 = 7000\ s^{-1}$ [101]. The back reaction is prevented in the presence of atmospheric oxygen, which rapidly oxidizes Ru(I). The yield of photooxidized heme *c* is 20% in a single flash.

Laser excitation of reduced yeast Ru_z-39-C*c* and yeast cyt bc_1 at 250 mM ionic strength led to rapid photooxidation of heme *c*, followed by electron transfer from cyt c_1 to oxidized heme *c* with a rate constant of $3900\ s^{-1}$, as monitored at 546 nm (Fig. 8) [101]. The oxidation of cyt c_1 was observed directly at 557 nm, which is an isobestic point for C*c*. A fast phase with a rate constant of $14{,}000\ s^{-1}$ was observed at ionic strengths below 150 mM due to electron transfer in a preformed Ru-39-C*c*:cyt bc_1 complex (Fig. 9). The rate constant of this intracomplex electron transfer reaction was independent of ionic strength from 5 mM to 120 mM, indicating that the complex does not change its configuration. Eq. (1) was used to calculate a theoretical rate constant for electron transfer from cyt c_1 to C*c* based on the X-ray crystal structure of the complex between yeast iso-1-C*c* and yeast cyt bc_1 [99] (Fig. 7). The calculated rate constant is between $1.8 \times 10^5\ s^{-1}$ and $3.3 \times 10^6\ s^{-1}$, assuming a reorganization energy λ between 0.7 and 1.0 V, and an edge-to-edge separation of 9.4 Å between the heme *c* and heme c_1 groups as given in the crystal structure. Although the theoretical value is larger than the experimental value of $1.4 \times 10^4\ s^{-1}$, the through-water jump of 4.5 Å between the two hemes in the crystallographic complex could give a large barrier to electron transfer that is not accounted for by Eq. (2).

Since both intracomplex and bimolecular phases are observed at 110 mM ionic strength, the bimolecular reaction involves formation of a 1:1 complex with rate constant $k_f = 2.0 \times 10^9\ M^{-1}\ s^{-1}$, intracomplex electron transfer with $k_{et} = 14{,}000\ s^{-1}$, and complex dissociation with $k_d = 1.7 \times 10^3\ s^{-1}$ [101]. The fast intracomplex phase disappears and the rate constant of the bimolecular phase increases to a maximum at 200 mM ionic strength (corresponding to $(I)^{1/2} = 0.45$ in $(M)^{1/2}$ units), indicating an increase in k_d (Fig. 9). The second-order rate constant decreases with increasing ionic strength above 250 mM ionic strength, consistent with a reaction between oppositely charged proteins (Fig. 9). Rajagukguk et al. [102] prepared a series of yeast Ru_z-39-C*c* mutants containing mutations of residues at the binding domain in order to characterize the interaction with cyt bc_1. The rate constants were measured using the ruthenium photooxidation technique at 250 mM, where the reaction is bimolecular (Table 5). The largest effect was observed for the R13A mutant, where the rate constant was decreased from $3500\ s^{-1}$ to $153\ s^{-1}$. This indicates that the π–cation interaction between yC*c* Arg-13 and Phe-230 of cyt c_1 observed in the crystal structure of the complex [99,100] is important for the reaction in solution. A substantial decrease in rate constant to $1090\ s^{-1}$ and $190\ s^{-1}$ for the K86A and K86D mutants, respectively, demonstrates that the charge–pair interaction between yCc Lys 86 and Glu 235 of cyt c_1 in the crystal structure is also important for the reaction in solution. Mutation of other yCc lysines to alanine, including 11, 72, 73, 79, and 87, also led to significant decreases in the rate constant (Table 5). Although there is only one electrostatic charge–pair interaction in the binding domain of the yCc:ybc_1 crystallographic complex, the 5 lysine amino groups on yC*c* and 5 carboxylate groups on cyt bc_1 immediately surrounding the interaction domain could guide C*c* to the binding site and contribute to complex formation [99,100].

Sarewicz et al. [103] carried out EPR studies indicating that the lifetime of the complex between *R. capsulatus* cyt c_2 and cyt bc_1 was longer than 100 μs at low ionic strength, decreasing to less than 400 ns at ionic strengths above 125 mM. Their results are consistent with a mechanism in which cyt c_2 binds rapidly to cyt bc_1 at low ionic strength allowing efficient intracomplex electron transfer, but product complex dissociation is slow, limiting enzyme turnover. At high ionic strength complex formation is slow and complex dissociation is so rapid that most collisions

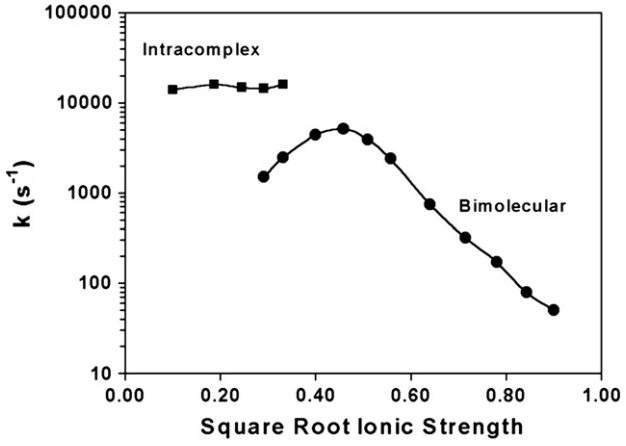

Fig. 9. Ionic strength dependence of the rate constant for photoinduced electron transfer between yeast Ru_z-39-C*c* and yeast cyt bc_1. The conditions were the same as in Fig. 8 except that 0 to 800 mM NaCl was present. The square root of ionic strength is in units of $[M]^{1/2}$.

Table 5
Reaction of yeast Ru-39-C*c* mutants with yeast cyt bc_1 [102]. The reaction solution contained 5 μM yeast Ru-39-C*c* mutant and 5 μM yeast cyt bc_1 in 5 mM sodium phosphate, pH 7.0 with 250 mM NaCl and 0.1% lauryl maltoside. The c_1 and *c* hemes were reduced with 10 μM ascorbate. The sequence numbering of horse C*c* is used.

Mutant	k (s^{-1})
None	3500
K11A	1480
T12A	2540
R13A	153
V28A	2620
K72A	1960
K73A	2190
K79A	1530
A81G	2400
K86A	1090
K86D	190
K87A	1120

do not result in electron transfer. At intermediate physiological ionic strength, complex formation and dissociation are both moderately rapid, and there is a moderate ratio of electron transfer per collision. The rapid kinetic studies discussed above [101] are also consistent with this mechanism. Sarewicz et al. [104] carried out EPR studies indicating that the dipole moment of cyt c_2 plays an important role in orienting the molecule for efficient electron transfer during the collision process.

The *P. denitrificans* cyt bc_1 complex contains just three subunits, the *b* subunit with heme b_L and heme b_H, the Rieske iron–sulfur protein (ISP), and cyt c_1 [105]. The cyt c_1 subunit has a tripartite domain structure consisting of a unique N-terminal acidic domain of 150 amino acids, a periplasmically oriented core domain containing the covalently attached heme *c*, and a C-terminal membrane anchor. The acidic domain may be analogous to the small acidic subunits of eukaryotic cyt bc_1, including the hinge protein of bovine cyt bc_1 and subunit 6 of yeast cyt bc_1 [106,107]. An unusual feature of *P. denitrificans* cyt bc_1 is that it has a "dimer of dimers" quaternary structure rather than the dimeric structure found in other cyt bc_1 complexes [108]. Cyt bc_1 transfers electrons to membrane-bound cyt c_{552} [109]. Kinetic studies have been carried out on genetically engineered soluble modules of both redox partners [110]. The soluble cytochrome c_1 core fragment (cyt c_{1CF}) consists of only the central core domain, without the acidic domain and the membrane anchor. The soluble cytochrome c_{552} fragment (cyt c_{552F}) contains only the C-terminal hydrophilic heme domain without the N-terminal membrane anchor and linker region. A new ruthenium cyt c_{552F} derivative (Ru_z-23-c_{552F}) was designed to measure rapid electron transfer with cyt c_{1CF} using the ruthenium photooxidation technique [110]. The bimolecular rate constant k_{12} decreased rapidly with increasing ionic strength above 40 mM, indicating that electrostatic interactions were important for the reaction between the two proteins. However, k_{12} was rapid, 3×10^9 M^{-1} s^{-1}, and nearly independent of ionic strength below 35 mM. These results are consistent with a two-step process involving very rapid formation of an initial complex guided by long-range electrostatic interactions, followed by short-range diffusion along the protein surfaces guided by hydrophobic interactions. No intracomplex electron transfer between Ru_z-23-c_{552F} and c_{1CF} was observed even at the lowest ionic strength, indicating a low-affinity complex. In contrast, yeast Ru_z-39-*Cc* formed a tight 1:1 complex with cyt c_{1CF} at ionic strengths below 60 mM with an intracomplex electron transfer rate constant of 50,000 s^{-1}. A group of cyt c_{1CF} mutants in the presumed docking site was generated based on information from the yeast cyt bc_1/cyt *c* co-crystal structure. Kinetic analysis of cyt c_{1CF} mutants located near the heme crevice provided preliminary identification of the interaction site for cyt c_{552F}, and suggest that formation of the encounter complex is guided primarily by the overall electrostatic surface potential rather than by defined ion pairs [110]. Ruthenium kinetic studies have shown that the acidic domain does not play a significant role in the reaction of cyt c_{552F} with *P. denitrificans* cyt bc_1 [111]. The reaction between a ruthenium horse C*c* derivatve and *R. sphaeroides* cyt bc_1 was found to have an intracomplex rate constant of 60,000 s^{-1} [112]. Mutagenesis studies indicated that acidic residues near the heme crevice of cyt c_1 are important in guiding C*c* to the binding domain [112].

5. Conclusions and future prospects

Extensive structural, spectroscopic, and kinetics studies have provided considerable insight into the mechanism of the cytochrome bc_1 complex. Most of the rate constants for the key electron transfer reactions have been measured for *R. sphaeroides* cyt bc_1 as indicated in Scheme 1 and Table 6. X-ray crystallographic and EPR studies have shown that inhibitors bound at the Q_o site affect the position and mobility of the ISP [8,10,17,25–28]. Kinetic studies have revealed that the reduction of cyt c_1 by 2Fe2S is rate-limited by the rotational diffusion of the ISP from the b-state to the c_1 state, and that the rate of this rotation is controlled by the type of inhibitor bound in the Q_o site [13,21,61,67,68]. On the basis of these studies it has been proposed that binding QH_2 to the Q_o site induces a conformational change in the *ef* and cd_1 loops leading to capture of the ISP in the b state and proton-coupled electron transfer from 2Fe2S to cyt c_1 [12,28]. Following electron transfer to cyt b_L and cyt b_H, the ISP is released from the b state, rotates to the c_1 state, and transfers an electron to cyt c_1. The detailed mechanism of how this bifurcated electron transfer reaction avoids short-circuit and bypass reactions remains enigmatic, however. A number of possibilities have been proposed, including control of the rotation of the ISP by the release of Q from the Q_o site or the reduction of cyt b_L and cyt b_H [12,28], double gating mechanisms [69,75–79], or coulombic gating of the motion of the semiquinone [72,77]. It has also been proposed that the reaction of Q at the Q_i site could affect the bifurcated reduction of QH_2 at the Q_o site and the motion of the ISP [26,27,84–89]. Moreover, experiments from several different laboratories indicate that electrons can be transferred between the two cyt b_L hemes in the homodimeric enzyme, suggesting that electrons can be distributed between the four quinone sites in the dimer [85,89–92]. However, it is not clear whether cross-monomer communication regulates reactions at the Q_o and Q_i sites. Future experiments are needed to address these important questions.

Table 6
Rate constants of reactions in *R. sphaeroides* cyt bc_1. Rate constants for the reactions shown in Scheme 1 were measured under the conditions reported in the references.

Reaction	Rate constant	References
$c_1 \rightarrow c$	$k_1 = 60{,}000\ s^{-1}$	[101,112]
$2Fe2S \rightarrow c_1$	$k_2 = 80{,}000\ s^{-1}$	[13,21,68]
$QH_2 \rightarrow 2Fe2S$	$k_3 = 2000\ s^{-1}$	[13,21,59,68]
$Q^{\bullet -} \rightarrow b_L$	$k_4 > 10^9\ s^{-1}$	[59]
$b_L \rightarrow b_H$	$k_5 = 10{,}000\ s^{-1}$	[60]
$b_H \rightarrow Q$	$k_6 > k_3$	[59]

Acknowledgements

This work was supported in part by NIH grants GM20488 and 8P30GM103450.

References

[1] B.L. Trumpower, R.B. Gennis, Energy transduction by cytochrome complexes in mitochondrial and bacterial respiration: the enzymology of coupling electron transfer reactions to transmembrane proton translocation, Annu. Rev. Biochem. 63 (1994) 675–716.
[2] B.L. Trumpower, The protonmotive Q cycle. Energy transduction by coupling of proton translocation to electron transfer by the cytochrome bc_1 complex, J. Biol. Chem. 265 (1990) 11409–11412.
[3] P. Mitchell, The protonmotive Q cycle: a general formulation, FEBS Lett. 59 (1975) 137–139.
[4] A.R. Crofts, The cytochrome bc_1 complex: function in the context of structure, Annu. Rev. Physiol. 66 (2004) 689–733.
[5] D. Xia, C.A. Yu, H. Kim, J.Z. Xia, A.M. Kachurin, L. Zhang, L. Yu, J. Deisenhofer, Crystal structure of the cytochrome bc_1 complex from bovine heart mitochondria, Science 277 (1997) 60–66.
[6] Z. Zhang, L. Huang, V.M. Shulmeister, Y.I. Chi, K.K. Kim, L.W. Hung, A.R. Crofts, E.A. Berry, S.H. Kim, Electron transfer by domain movement in cytochrome bc_1, Nature 392 (1998) 677–684.
[7] S. Iwata, J.W. Lee, K. Okada, J.K. Lee, M. Iwata, B. Rasmussen, T.A. Link, S. Ramaswamy, B.K. Jap, Complete structure of the 11-subunit bovine mitochondrial cytochrome bc_1 complex, Science 281 (1998) 64–71.
[8] H. Kim, D. Xia, C.A. Yu, J.Z. Xia, A.M. Kachurin, L. Zhang, L. Yu, J. Deisenhofer, Inhibitor binding changes domain mobility in the iron–sulfur protein of the mitochondrial bc_1 complex from bovine heart, Proc. Natl. Acad. Sci. U. S. A. 95 (1998) 8026–8033.
[9] C. Hunte, J. Koepke, C. Lange, T. Rossmanith, H. Michel, Structure at 2.3 Å resolution of the cytochrome bc_1 complex from the yeast *Saccharomyces cerevisiae* co-crystallized with an antibody Fv fragment, Struct. Fold. Des. 8 (2000) 669–684.
[10] L. Esser, M. Elberry, F. Zhou, C.A. Yu, L. Yu, D. Xia, Inhibitor-complexed structures of the cytochrome bc_1 from the photosynthetic bacterium *Rhodobacter sphaeroides*, J. Biol. Chem. 283 (2008) 2846–2857.

[11] E.A. Berry, L.S. Huang, L.K. Saechao, N.G. Pon, M. Valkova-Valchanova, F. Daldal X-Ray, Structure of *Rhodobacter capsulatus* cytochrome bc_1: comparison with its mitochondrial and chloroplast counterparts, Photosynth. Res. 81 (2004) 251–275.

[12] D. Xia, L. Esser, L. Yu, C.A. Yu, Structural basis for the mechanism of electron bifurcation at the quinol oxidation site of the cytochrome bc_1 complex, Photosynth. Res. 92 (2007) 17–34.

[13] R.C. Sadoski, G. Engstrom, H. Tian, L. Zhang, C.A. Yu, L. Yu, B. Durham, F. Millett, Use of a photoactivated ruthenium dimer complex to measure electron transfer between the Rieske iron–sulfur protein and cytochrome c_1 in the cytochrome bc_1 complex, Biochemistry 39 (2000) 4231–4236.

[14] H. Tian, L. Yu, M.W. Mather, C.A. Yu, Flexibility of the neck region of the Rieske iron–sulfur protein is functionally important in the cytochrome bc_1 complex, J. Biol. Chem. 273 (1998) 27953–27959.

[15] K. Xiao, L. Yu, C.A. Yu, Confirmation of the involvement of protein domain movement during the catalytic cycle of the cytochrome bc_1 complex by the formation of an intersubunit disulfide bond between cytochrome *b* and the iron–sulfur protein, J. Biol. Chem. 275 (2000) 38597–38604.

[16] H. Tian, S. White, L. Yu, C.A. Yu, Evidence for the head domain movement of the Rieske iron–sulfur protein in electron transfer reaction of the cytochrome bc_1 complex, J. Biol. Chem. 274 (1999) 7146–7152.

[17] E. Darrouzet, M. Valkova-Valchanova, F. Daldal, Probing the role of the Fe–S subunit hinge region during Q_o site catalysis in *Rhodobacter capsulatus* bc_1 complex, Biochemistry 39 (2000) 15475–15483.

[18] E. Darrouzet, M. Valkova-Valchanova, C.C. Moser, P.L. Dutton, F. Daldal, Uncovering the 2Fe2S domain movement in cytochrome bc_1 and its implications for energy conversion, Proc. Natl. Acad. Sci. U. S. A. 97 (2000) 4567–4572.

[19] J.H. Nett, C. Hunte, B.L. Trumpower, Changes to the length of the flexible linker region of the Rieske protein impair the interaction of ubiquinol with the cytochrome bc_1 complex, Eur. J. Biochem. 267 (2000) 5777–5782.

[20] M. Ghosh, Y. Wang, C.E. Ebert, S. Vadlamuri, D.S. Beattie, Substituting leucine for alanine-86 in the tether region of the iron–sulfur protein of the cytochrome bc_1 complex affects the mobility of the 2Fe2S domain, Biochemistry 40 (2001) 327–335.

[21] G. Engstrom, K. Xiao, C.A. Yu, L. Yu, B. Durham, F. Millett, Photoinduced electron transfer between the Rieske iron–sulfur protein and cytochrome c_1 in the *Rhodobacter sphaeroides* cytochrome bc_1 complex. Effects of pH, temperature, and driving force, J. Biol. Chem. 277 (2002) 31072–31078.

[22] E. Darrouzet, M. Valkova-Valchanova, F. Daldal, The [2Fe2S] cluster E_m as an indicator of the iron–sulfur subunit position in the ubihydroquinone oxidation site of the cytochrome bc_1 complex, J. Biol. Chem. 277 (2002) 3464–3470.

[23] E. Darrouzet, F. Daldal, Movement of the iron–sulfur subunit beyond the *ef* loop of cytochrome b is required for multiple turnovers of the bc_1 complex but not for single turnover Q_o site catalysis, J. Biol. Chem. 277 (2002) 3471–3476.

[24] M. Brugna, S. Rodgers, A. Schricker, G. Montoya, M. Kazmeier, W. Nitschke, I. Sinning, A spectroscopic method for observing the domain movement of the Rieske iron–sulfur protein, Proc. Natl. Acad. Sci. U. S. A. 97 (2000) 2069–2074.

[25] E.A. Berry, L.S. Huang, Conformationally linked interaction in the cytochrome bc_1 complex between inhibitors of the Q_o site and the Rieske iron–sulfur protein, Biochim. Biophys. Acta 1807 (2011) 1349–1363.

[26] J.W. Cooley, A.G. Roberts, M.K. Bowman, D.M. Kramer, F. Daldal, The raised midpoint potential of the 2Fe2S cluster of cytochrome bc_1 is mediated by both the Qo site occupants and the head domain position of the Fe–S protein subunit, Biochemistry 43 (2004) 2217–2227.

[27] M. Sarewicz, M. Dutka, W. Froncisz, A. Osyczk, Magnetic interactions sense changes in distance between heme b_L and the iron–sulfur cluster in cytochrome bc_1, Biochemistry 48 (2009) 5708–5720.

[28] L. Esser, X. Gong, S. Yang, L. Yu, C.A. Yu, D. Xia, Surface-modulated motion switch: capture and release of iron–sulfur protein in the cytochrome bc_1 complex, Proc. Natl. Acad. Sci. U. S. A. 103 (2006) 13045–13050.

[29] K. Kalyanasundaram, Photochemistry of Polypyridine and Porphyrin Complexes, Academic Press, London, 1992.

[30] L.P. Pan, B. Durham, J. Wolinska, F. Millett, Preparation and characterization of singly labeled ruthenium polypyridine cytochrome *c* derivatives, Biochemistry 27 (1988) 7180–7184.

[31] B. Durham, L.P. Pan, J. Long, F. Millett, Photoinduced electron-transfer kinetics of singly labeled ruthenium bis-(bipyridine) dicarboxybipyridine cytochrome *c* derivatives, Biochemistry 28 (1989) 8659–8665.

[32] R.-Q. Liu, L. Geren, P. Anderson, J.L. Fairris, N. Peffer, A. McKee, B. Durham, F. Millett, Design of ruthenium-cytochrome *c* derivatives to measure electron transfer to cytochrome *c* peroxidase, Biochimie 77 (1995) 549–561.

[33] B. Durham, L.P. Pan, S. Hahm, J. Long, F. Millett, Electron transfer in biology and the solid state, in: M.K. Johnson, et al., (Eds.), ACS Advances in Chemistry Series, American Chemical Society, Washington, D. C., 1990, pp. 181–193.

[34] L. Geren, S. Hahm, B. Durham, F. Millett, Photoinduced electron transfer between cytochrome *c* peroxidase and yeast cytochrome *c* labeled at Cys 102 with (4-bromomethyl-4′-methylbipyridine)[bis(bipyridine)]ruthenium, Biochemistry 30 (1991) 9450–9457.

[35] A. Willie, P.S. Stayton, S.G. Sligar, B. Durham, F. Millett, Genetic engineering of redox donor sites: measurement of intracomplex, electron transfer between ruthenium-65-cytochrome b_5 and cytochrome *c*, Biochemistry 31 (1992) 7237–7242.

[36] L.M. Geren, J.R. Beasley, B.R. Fines, A.J. Saunders, S. Hibdon, G.J. Pielak, B. Durham, F. Millett, Design of a ruthenium-cytochrome *c* derivative to measure the electron transfer to the initial acceptor in cytochrome *c* oxidase, J. Biol. Chem. 270 (1995) 2466–2472.

[37] K. Wang, H. Mei, L. Geren, M.A. Miller, A. Saunders, X. Wang, J.L. Waldner, G.J. Pielak, B. Durham, F. Millett, Design of a ruthenium-cytochrome *c* derivative to measure electron transfer to the radical cation and oxyferryl heme in cytochrome *c* peroxidase, Biochemistry 35 (1996) 15107–15119.

[38] D. Zaslavsky, R.C. Sadoski, K. Wang, B. Durham, R.B. Gennis, F. Millett, Single electron reduction of cytochrome *c* oxidase compound F: resolution of partial steps by transient spectroscopy, Biochemistry 37 (1998) 14910–14916.

[39] S.E. Brand, S. Rajagukguk, K. Ganesan, L. Geren, M. Fabian, D. Han, R.B. Gennis, B. Durham, F. Millett, A new ruthenium complex to study single-electron reduction of the pulsed OH state of detergent-solubilized cytochrome oxidase, Biochemistry 46 (2007) 14610–14618.

[40] J.R. Winkler, D.G. Nocera, K.M. Yocom, E. Bordignon, H.B. Gray, Electron-transfer kinetics of Ru(NH3)5(III)(His-33)-ferricytochrome *c*, J. Am. Chem. Soc. 104 (1982) 5798–5800.

[41] S.S. Isied, G. Worosila, S.J. Atherton, Electron transfer across polypeptides. Intramolecular electron transfer from ruthenium (II) to iron (III) in histidine-33 modified horse heart cytochrome *c*, J. Am. Chem. Soc. 104 (1982) 7659–7661.

[42] J.R. Scott, J.L. Fairris, M. McLean, K. Wang, S.G. Sligar, B. Durham, F. Millett, Intramolecular electron-transfer reactions of cytochrome b_5 covalently bonded to ruthenium(II) polypyridine complexes: reorganizational energy and pressure effects, Inorg. Chim. Acta 243 (1996) 193.

[43] J.L. Fairris, K. Wang, L. Geren, G.J. Pielak, B. Durham, F. Millett, Intramolecular electron transfer in yeast cytochrome *c* covalently bonded to ruthenium(II) polypyridine complexes at Cys39, in: ACS Advances in Chemistry Series, 254, Photochemistry and Radiation Chemistry, ACS, Washington, DC, 1998, pp. 99–110.

[44] F. Millett, B. Durham, Design of photoactive ruthenium complexes to study interprotein electron transfer, Biochemistry 41 (2002) 11315–11324.

[45] T.J. Meade, H.B. Gray, J.R. Winkler, Driving-force effects on the rate of long-range electron transfer in ruthenium-modified cytochrome *c*, J. Am. Chem. Soc. 111 (1989) 4353–4356.

[46] I.-J. Chang, H.B. Gray, J.R. Winkler, High-driving force electron transfer in metalloproteins: intramolecular oxidation of ferrocytochrome *c* by Ru(2,2′ bpy)2(im)(His-33)3+, J. Am. Chem. Soc. 113 (1991) 7056–7757.

[47] D.S. Wuttke, M.J. Bjerrum, J.R. Winkler, H.B. Gray, Electron-tunneling pathways in cytochrome *c*, Science 256 (1992) 1007–1009.

[48] A.J. Di Bilio, C. Dennison, H.B. Gray, B.E. Ramirez, A.G. Sykes, J.R. Winkler, Electron transfer in ruthenium-modified plastocyanin, J. Am. Chem. Soc. 120 (1998) 7551–7556.

[49] M.J. Bjerrum, D.R. Casimiro, I. Chang, A.J. De Bilio, H.B. Gray, M.G. Hill, R. Langen, G.A. Mines, L.K. Skov, J.R. Winkler, D.S. Wuttke, Electron transfer in ruthenium-modified proteins, J. Bioenerg. Biomembr. 27 (1995) 295–302.

[50] R.A. Marcus, On the theory of oxidation–reduction reactions involving electron transfer, J. Chem. Phys. 24 (1956) 966–978.

[51] C.C. Moser, J.M. Keske, K. Warncke, R.S. Farid, P.L. Dutton, Nature of biological electron transfer, Nature 355 (1992) 796–802.

[52] C.A. Yu, L. Yu, T.E. King, Kinetics of electron transfer between cardiac cytochrome c_1 and *c*, J. Biol. Chem. 248 (1973) 528–533.

[53] S. De Vries, S.P.J. Albracht, J.A. Berden, E.C. Slater, The pathway of electron through QH_2:cytochrome c oxidoreductase studied by pre-steady-state kinetics, Biochim. Biophys. Acta 681 (1982) 41–53.

[54] K.C. Hansen, B.E. Schultz, F. Wang, S.I. Chan, Reaction of *E. coli* cytochrome bo_3 and mitochondrial cytochrome bc_1 with a photoreleasable decylubiquinol, Biochim. Biophys. Acta 1456 (2000) 121–137.

[55] C.H. Snyder, E.B. Guierrez-Cirlos, B.L. Trumpower, Evidence for a concerted mechanism of ubiquinol oxidation by the cytochrome bc_1 complex, J. Biol. Chem. 275 (2000) 13555-13541.

[56] B.L. Trumpower, A concerted, alternating sites mechanism of ubiquinol oxidation by the dimeric cytochrome bc_1 complex, Biochim. Biophys. Acta 1555 (2002) 166–173.

[57] A.R. Crofts, S.W. Meinhardt, A Q-cycle mechanism for the cyclic electron transfer chain of *Rp. sphaeroides*, Biochem. Soc. Trans. 10 (1982) 201–203.

[58] S.W. Meinhardt, A.R. Crofts, Kinetic and thermodynamic resolution of cytochrome c_1 and cytchrome c_2 from *Rhodopseudomonas sphaeroides*, FEBS Lett. 149 (1982) 223–227.

[59] A.R. Crofts, Z. Wang, How rapid are the internal reactions of the ubiquinol: cytochrome c_2 oxidoreductase? Photosynth. Res. 22 (1989) 69–87.

[60] V.P. Shinkarev, A.R. Crofts, C.A. Wraight, The electric field generated by photosynthetic reaction center induces rapid reversed electron transfer in the bc_1 complex, Biochemistry 40 (2001) 12584–12590.

[61] J. Havens, M. Castellani, T. Kleinschroth, B. Ludwig, B. Durham, F. Millett, Photoinitiated electron transfer within the *Paracoccus denitrificans* cytochrome bc_1 complex: mobility of the iron–sulfur protein is modulated by the occupant of the Q_o site, Biochemistry 50 (2011) 10462–10472.

[62] T.A. Link, Two pK values of the oxidized Rieske [2Fe2S] cluster observed by CD spectroscopy, Biochim. Biophys. Acta 1185 (1994) 81–84.

[63] N.B. Ugulava, A.R. Crofts, CD-monitored redox titration of the Rieske Fe–S protein of *Rb. sphaeroides*: pH dependence of the midpoint potential in isolated bc_1 complex and in membranes, FEBS Lett. 440 (1998) 409–413.

[64] M. Ritter, H. Palsdottir, M. Abe, W. Mäntele, C. Hunte, H. Miyoshi, P. Hellwig, Direct evidence for the interaction of stigmatellin with a protonated acidic group in the bc_1 complex from *Saccharomyces cerevisiae* as monitored by FTIR difference spectroscopy and ^{13}C specific labeling, Biochemistry 43 (2004) 8439–8446.

[65] L. Esser, B. Quinn, Y.F. Li, M. Zhang, M. Elberry, L. Yu, C.A. Yu, D. Xia, Crystallographic studies of quinol oxidation site inhibitors: a modified classification of inhibitors for the cytochrome bc_1 complex, J. Mol. Biol. 341 (2004) 281–302.

[66] C.R. Lancaster, C. Hunte, J. Kelley, B.L. Trumpower, R. Ditchfield, A comparison of stigmatellin conformations, free and bound to the photosynthetic reaction center and the cytochrome bc_1 complex, J. Mol. Biol. 368 (2007) 197–208.

[67] K. Xiao, G. Engstrom, S. Rajagukguk, C.A. Yu, L. Yu, B. Durham, F. Millett, Effect of famoxadone on photoinduced electron transfer between the iron–sulfur center and cytochrome c_1 in the cytochrome bc_1 complex, J. Biol. Chem. 278 (2003) 11419–11426.

[68] S. Rajagukguk, S. Yang, C.A. Yu, L. Yu, B. Durham, F. Millett, Effect of mutations in the cytochrome *b ef* loop on the electron-transfer reactions of the Rieske iron–sulfur protein in the cytochrome bc_1 complex, Biochemistry 46 (2007) 1791–1798.

[69] A. Osyczka, C.C. Moser, F. Daldal, P.L. Dutton, Reversible redox energy coupling in electron transfer chains, Nature 427 (2004) 607–612.

[70] S.E. Chobot, H. Zhang, C.C. Moser, P.L. Dutton, Breaking the Q-cycle: finding new ways to study Q_o through thermodynamic manipulations, J. Bioenerg. Biomembr. 40 (2008) 501–507.

[71] S. Hong, N. Ugulava, M. Guergova-Kuras, A.R. Crofts, The energy landscape for ubihydroquinone oxidation at the Q_o site of the bc_1 complex in *Rhodobacter sphaeroides*, J. Biol. Chem. 274 (1999) 33931–33944.

[72] A.R. Crofts, S. Hong, Z. Zhangand, E.A. Berry, Physicochemical aspects of the movement of the Rieske iron sulfur protein during quinol oxidation by the bc_1 complex from mitochondria and photosynthetic bacteria, Biochemistry 38 (1999) 15827–15839.

[73] S. Lhee, D. Kolling, S. Nair, S. Dikanov, A.R. Crofts, Modifications of protein environment of the [2Fe2S] cluster of the bc_1 complex: effects on the biophysical properties of the Rieske iron–sulfur protein and on the kinetics of the complex, J. Biol. Chem. 285 (2010) 9233–9248.

[74] E. Darrouzet, F. Daldal, Protein–protein interactions between cytochrome *b* and the Fe–S protein subunits during QH_2 oxidation and large-scale domain movement in the bc_1 complex, Biochemistry 42 (2003) 1499–1507.

[75] P.R. Rich, The quinone chemistry of *bc* complexes, Biochim. Biophys. Acta 1658 (2004) 165–171.

[76] A. Osyczka, C.C. Moser, P.L. Dutton, Fixing the Q cycle, Trends Biochem. Sci. 30 (2005) 176–182.

[77] A.R. Crofts, S. Lhee, S.B. Crofts, J. Cheng, S. Rose, Proton pumping in the bc_1 complex: a new gating mechanism that prevents short circuits, Biochim. Biophys. Acta 1757 (2006) 1019–1034.

[78] A.Y. Mulkidjanian, Ubiquinol oxidation in the cytochrome bc_1 complex: reaction mechanism and prevention of short-circuiting, Biochim. Biophys. Acta 1709 (2005) 5–34.

[79] A. Osyczka, H. Zhang, C. Mathé, P.R. Rich, C.C. Moser, P.L. Dutton, Role of the PEWY glutamate in hydroquinone–quinone oxidation–reduction catalysis in the Q_o Site of cytochrome bc_1, Biochemistry 45 (2006) 10492–10503.

[80] J. Zhu, T. Egawa, S.R. Yeh, L. Yu, C.A. Yu, Simultaneous reduction of iron–sulfur protein and cytochrome b_L during ubiquinol oxidation in cytochrome bc_1 complex, Proc. Natl. Acad. Sci. U. S. A. 104 (2007) 4864–4869.

[81] J.L. Cape, M.K. Bowman, D.M. Kramer, A semiquinone intermediate generated at the Q_o site of the cytochrome bc_1 complex: importance for the Q-cycle and superoxide production, Proc. Natl. Acad. Sci. U. S. A. 104 (2007) 7887–7892.

[82] H. Zhang, A. Osyczka, P.L. Dutton, C.C. Moser, Exposing the complex III Q_o semiquinone radical, Biochim. Biophys. Acta 1767 (2007) 883–887.

[83] I. Forquer, R. Covian, M.K. Bowman, B.L. Trumpower, D.M. Kramer, Similar transition states mediate the Q-cycle and superoxide production by the cytochrome bc_1 complex, J. Biol. Chem. 281 (2006) 38459–38465.

[84] R. Covian, B.L. Trumpower, Regulatory interactions in the dimeric cytochrome bc_1 complex: the advantages of being a twin, Biochim. Biophys. Acta 1777 (2008) 1079–1091.

[85] M. Castellani, R. Covian, T. Kleinschroth, O. Anderka, B. Ludwig, B. Trumpower, Direct demonstration of half-of-the-sites reactivity in the dimeric cytochrome bc_1 complex: enzyme with one inactive monomer is fully active but unable to activate the second ubiquinol oxidation site in response to ligand binding at the ubiquinone reduction site, J. Biol. Chem. 285 (2010) 502–510.

[86] J. Cooley, A structural model for across membrane coupling between the Q_o and Q_i active sites of cytochrome bc_1, Biochim. Biophys. Acta 1797 (2010) 1842–1848.

[87] A.Y. Mulkidjanian, Proton translocation by the cytochrome bc_1 complexes of phototrophic bacteria: introducing the activated Q-cycle, Photochem. Photobiol. Sci. 6 (2007) 19–34.

[88] X. Cen, L. Yu, C.A. Yu, Domain movement of iron sulfur protein in cytochrome bc_1 complex is facilitated by the electron transfer from cytochrome b_L to b_H, FEBS Lett. 582 (2008) 523–526.

[89] P. Lanciano, D.W. Lee, H. Yang, E. Darrouzet, F. Daldal, Intermonomer electron transfer between the low-potential *b* hemes of cytochrome *bc* , Biochemistry 50 (2011) 1651–1663.

[90] M. Świerczek, E. Cieluch, M. Sarewicz, A. Borek, C.C. Moser, P.L. Dutton, A. Osyczka, An electronic bus bar lies in the core of cytochrome bc_1, Science 329 (2010) 451–454.

[91] M. Czapla, A. Borek, M. Sarewicz, A. Osyczka, Enzymatic activities of isolated cytochrome *bc* -like complexes containing fused cytochrome b subunits with asymmetrically inactivated segments of electron transfer chains, Biochemistry 51 (2012) 829–835.

[92] S. Hong, D. Victoria, A.R. Crofts, Inter-monomer electron transfer is too slow to compete with monomeric turnover in bc_1 complex, Biochim. Biophys. Acta 1817 (2012) 1053–1062.

[93] A.J. Ahmed, H.T. Smith, M.B. Smith, F. Millett, Effect of specific lysine modification on the reduction of cytochrome *c* by succinate-cytochrome *c* reductase, Biochemistry 17 (1978) 2479–2483.

[94] H. Smith, A. Ahmed, F. Millett, Electrostatic interaction of cytochrome *c* with cytochrome c_1 and cytochrome oxidase, J. Biol. Chem. 256 (1981) 4984–4990.

[95] S.H. Speck, S. Ferguson-Miller, N. Osheroff, E. Margoliash, Definition of cytochrome *c* binding domains by chemical modification: kinetics of reaction with beef mitochondrial reductase, Proc. Natl. Acad. Sci. U. S. A. 76 (1979) 155–160.

[96] B.W. Konig, N. Osheroff, J. Wilms, A.O. Muijsers, H.L. Dekker, E. Margoliash, Mapping of the interaction domain for purified cytochrome c_1 on cytochrome *c*, FEBS Lett. 111 (1980) 359–398.

[97] J. Stonehuerner, P. O'Brien, L. Geren, F. Millett, J. Steidl, L. Yu, C.-A. Yu, Identification of the binding site on cytochrome c_1 for cytochrome *c*, J. Biol. Chem. 260 (1983) 5392–5398.

[98] H.E. Gutweniger, C. Grassi, C. Bisson, Interaction between cytochrome *c* and ubiquinone–cytochrome *c* oxidoreductase: a study with water-soluble carbodiimides, Biochem. Biophys. Res. Commun. 116 (1983) 272–283.

[99] C. Lange, C. Hunte, Crystal structure of the yeast cytochrome bc_1 complex with its bound substrate cytochrome c, Proc. Natl. Acad. Sci. U. S. A. 99 (2002) 2800–2805.

[100] S.R.N. Solmaz, C. Hunte, Structure of complex III with bound cytochrome *c* in reduced state and definition of a minimal core interface for electron transfer, J. Biol. Chem. 283 (2008) 17542–17549.

[101] G. Engstrom, R. Rajagukguk, A.J. Saunders, C. Patel, S. Rajagukguk, T. Merbitz-Zahradnik, K. Xiao, G. Pielak, B. Trumpower, C.-A. Yu, L. Yu, B. Durham, F. Millett, Design of a ruthenium-labeled cytochrome *c* derivative to study electron transfer with the cytochrome bc_1 complex, Biochemistry 42 (2003) 2816–2824.

[102] S. Rajagukguk, Synthesis and use of Ruthenium Complexes in the Study of Electron Transfer Reactions within the Cytochrome bc_1 Complex and with its redox partner cytochrome *c*, Ph.D. Dissertation, University of Arkansas, 2006.

[103] M. Sarewicz, A. Bork, F. Daldal, W. Froncisz, A. Osyczka, Demonstration of short-lived complexes of cytochrome *c* with cytochrome bc_1 by EPR spectroscopy, J. Biol. Chem. 283 (2008) 24826–24836.

[104] M. Sarewicz, R. Pietras, W. Froncisz, A. Osyczka, Reorientation of cytochrome c_2 upon interaction with oppositely charged macromolecules probed by SR EPR: implications for the role of dipole moment to facilitate collisions in proper configuration for electron transfer, Metallomics 3 (2011) 404–409.

[105] B. Kurowski, B. Ludwig, The genes of the *Paracoccus denitrificans* bc_1 complex. Nucleotide sequence and homologies between bacterial and mitochondrial subunits, J. Biol. Chem. 262 (1987) 13805–13811.

[106] C.H. Kim, C. Balny, T.E. King, Role of the hinge protein in the electron transfer between cardiac cytochrome c_1 and *c*. Equilibrium constants and kinetic probes, J. Biol. Chem. 262 (1987) 8103–8108.

[107] M.E. Schmitt, B.L. Trumpower, Subunit 6 regulates half-of-the-sites reactivity of the dimeric cytochrome bc_1 complex in *Saccharomyces cerevisiae*, J. Biol. Chem. 265 (1990) 17005–17011.

[108] N. Morgner, T. Kleinschroth, H.D. Barth, B. Ludwig, B. Brutschy, A novel approach to analyze membrane proteins by laser mass spectrometry: from protein subunits to the integral complex, J. Am. Soc. Mass Spectrom. 18 (2007) 1429–1438.

[109] A. Turba, M. Jetzek, B. Ludwig, Purification of *Paracoccus denitrificans* cytochrome c_{552} and sequence analysis of the gene, Eur. J. Biochem. 231 (1995) 259–265.

[110] J. Janzon, Q. Yuan, F. Malatesta, P. Hellwig, B. Ludwig, B. Durham, F. Millett, Probing the *Paracoccus denitrificans* cytochrome c_1–cytochrome c_{552} interaction by mutagenesis and fast kinetics, Biochemistry 47 (2008) 12974–12984.

[111] M. Castellani, J. Havens, T. Kleinschroth, F. Millett, B. Durham, F. Malatesta, B. Ludwig, The acidic domain of cytochrome *c* in *Paracoccus denitrificans*, analogous to the acidic subunits in eukaryotic *bc* complexes, is not involved in the electron transfer reaction to its native substrate cytochrome c_{552}, Biochim. Biophys. Acta 1807 (2011) 1383–1389.

[112] H. Tian, R. Sadoski, L. Zhang, C.-A. Yu, L. Yu, B. Durham, F. Millett, Definition of the interaction domain for cytochrome *c* on the cytochrome bc_1 complex. Steady-state and rapid kinetic analysis of electron transfer between cytochrome *c* and *Rhodobacter sphaeroides* cytochrome bc_1 surface mutants, J. Biol. Chem. 275 (2000) 9587–9595.